Supplementary Online Material

Supplementary Results

Decreased GPx Activity in GPx1$^{-/-}$/ApoE$^{-/-}$ mice. GPx activity was decreased 17-fold in the heart, 12-fold in the aorta, 14-fold in the vena cava but not in plasma of *GPx1$^{-/-}$/ApoE$^{-/-}$* mice compared with *GPx1$^{+/+}$/ApoE$^{-/-}$* (**Supplementary Fig. I**). Total cholesterol, triglyceride levels, and body weights were similar in *GPx1$^{-/-}$/ApoE$^{-/-}$* and *GPx1$^{+/+}$/ApoE$^{-/-}$* mice (**Supplementary Table I**).

***GPX1 and ROS1* variants.** The *GPX1* single nucleotide variant rs1050450 is associated with C to T substitution in exon 2 resulting in the substitution of proline for leucine at codon 198. This substitution leads to reduced enzymatic function through conformational changes related to the absence of a free amino group on the alpha carbon atom.(1) The *ROS1* rs529038 is associated with a G to A substitution in exon 42 leading to a change from aspartic acid to asparagine at position 2213 in the protein kinase domain near to cytoplasmic phosphorylation sites. The function of this mutation is currently unknown.

Supplemental Experimental Procedures

Animals

Mice were maintained in temperature-controlled (20°C to 22°C) cages with a 12-hour light-dark cycle. Sterile water and standard chow diet were available *ad libitum*. Mice with constitutive deletion of *GPx1* (*GPx1$^{-/-}$,* a kind gift of Dr Ye Shi-Ho), were crossed with C57BL/6J *ApoE$^{-/-}$* mice (Jackson Laboratories, Bar Harbor, MI) producing heterozygote *GPx1-* breeders. These breeders were mated with *ApoE$^{-/-}$* mice to produce *GPx1$^{-/-}$/ApoE$^{-/-}$* and *GPx1$^{+/+}$/ApoE$^{-/-}$* littermates. Some of these mice were further cross-bred with Transgenic Tie2-*LacZ* mice (Jackson Laboratories, Bar Harbor, MI) expressing β-Gal localized to the nucleus of endothelial cells.(2) Heterozygote *GPx1$^{+/-}$/ApoE$^{-/-}$/LacZ^{+}* mice were mated with *ApoE$^{-/-}$* homozygotes to produce experimental *GPx1$^{+/+}$/ApoE$^{-/-}$, GPx1$^{+/+}$/ApoE$^{-/-}$/LacZ^{+}, GPx1$^{-/-}$/ApoE$^{-/-}$*, and *GPx1$^{-/-}$/ApoE$^{-/-}$/LacZ^{+}* mice. In the genistein treated group, animals received genistein 30mg/kg

subcutaneously daily post-procedure until sacrifice. In the crizotinib treated group, animals received crizotinib 100mg/kg by gavage daily post-procedure until sacrifice. In the rapamycin treated group animals received rapamycin 2mg/kg by intra-peritoneal injection daily post-procedure until sacrifice.(3) In the glutathione mono-ethyl ester treated group animals received 10mmol/kg/day intraperitoneal daily post-procedure until sacrifice. Animal care was provided in accordance with the Laboratory Animal Welfare Act, the Guide for the Care and Use of Laboratory Animals (National Institutes of Health, publication 78-23, revised 1978) and the Stanford University School of Medicine guidelines and policies for the use of laboratory animals for research and teaching.

Genotype determination.

DNA was obtained by extraction from mouse tail or earsnips. DNA (1 μl) was amplified in a 50-μl PCR reaction containing 10 mM Tris · HCl (pH 8.3), 50 mM KCl, 1.5 mM $MgCl_2$, 0.001% gelatin, 0.1 mM dNTP, and 0.18 μM each primer. To identify the WT *GPX1* gene, we utilized the forward primer FinN (5′-GTTTCCCGTGCAATCAGTTCG-3′) and the reverse primer R_3N (5′-TCGGACGTACCCTTGAGGGAAT-3′) to detect the presence of a 293-bp fragment. To identify *GPx-1*$^{-/-}$ mice, we used FinN and RpgkN (5′-CATTTGTCACGTCCTGCAC-3′) as the reverse primer to amplify a 509-bp fragment in the NEO insert. Genotypes of *LacZ*$^{-/-}$, $^{+/-}$, $^{+/+}$ and mice were identified using The Jackson Laboratory's PCR protocol (primers, 5′-ATCCTCTGCATGGTCAGGTC-3′ and 5′-CGT-GGCCTGATTCATTCC-3′). For *ApoE*$^{-/-}$ mice genotyping, a similar protocol was used with primers: oIMR180 5′-GCCTAGCCGAGGGAGAGCCG-3′, oIMR181 5′-TGTGACT-TGGGAGCTCTGCAGC-3′, and oIMR182 5′-GCCGCCCCG-ACTGCATCT-3′. For *LacZ* Reaction products were analyzed by electrophoresis on a 1% agarose gel. *GPx-1*$^{-/-}$ mice were identified by an exclusive 509-bp product, and WT mice were identified by an exclusive 293-bp product.

Gene expression analysis

Tissue from human coronary artery atherectomy samples (n=89) or *ApoE*$^{-/-}$*/C57Bl6J* wild-type mice at 24 weeks (n=15 mice/group) was used for RNA isolation. Custom microarrays were developed by our laboratory in collaboration with Agilent Technologies (Palo Alto, California) for human samples and the Stanford Microarray Core (for mouse samples).(4) RNA was isolated using standard techniques based on guanidium thiocyanate as described previously.(4) Extensive quality control testing of all RNA was carried out. Samples were quantified with the NanoDrop ND-1000 Spectrophotometer (NanoDrop, Wilmington, DE), and RNA integrity was assessed with the 2100 Bioanalyzer System and RNA 6000 Pico LabChip Kit (Agilent Technologies). For human samples, array image acquisition and feature extraction was performed using the Agilent G2565AA Microarray Scanner and feature extraction software version A.6.1.1. Normalization was performed using a LOWESS algorithm, and dye-normalized signals were used in calculating log ratios. For significance analysis of microarrays (SAM), a K-nearest-neighbor algorithm was applied to impute for missing values. SAM was used to identify genes with statistically different expression. Heatmaps were generated using the HeatMap Builder software developed by our laboratory (http://ashleylab.stanford.edu/tools_scripts.html).

Network Analysis

We performed network analysis of human in-stent stenosis as described previously.[3] Briefly, rotational coronary atherectomy was performed in 89 patients, 55 with de novo atherosclerosis and 34 with in-stent stenosis. The derived tissue was divided and subjected to either RNA isolation or fixation for histological analysis. Following hybridization of the resulting RNA to a 22,000 probe oligonucleotide microarray (designed by the authors) the expression profile of *de novo* atherosclerosis was compared to that of in-stent stenosis as described above. Independently, biological networks were generated from the literature using text mining as described previously.[2] In brief, the text mining approach was developed in collaboration with the Agilent network biology team and is freely accessible via the Agilent Literature

Search app (Version 2.0) in Cytoscape (www.cytoscape.com).(5-9) Gene names and aliases genome wide are mapped to microarray gene identifications. Text for the entire abstracted literature (Pubmed) is interrogated for occurrences of these gene names or aliases. If a gene or alias is found in a sentence with another gene or alias, a text search of the intervening words is carried out for activator verbs such as 'inhibits', 'regulates', 'controls'. If a verb in this lexicon is found, then an interaction is created in Cytoscape, consisting of the two genes (nodes) and an edge between them. A biological network in Cytoscape (version 2.8)[4] is built from these pathway interactions. The discovered networks conform to scale free topology. Using a separate program, we derive mean difference statistics for each gene from the Significance Analysis of Microarrays. Significance for each sub-network is calculated and displayed both as the cumulative or mean d statistic for all the members of the network.[5]

Tissue Glutathione and Cellular GPx-1 Activity

Tissue concentrations of glutathione (total, reduced, and oxidized) were measured in aortic or stented aortic homogenates, after deproteinization with metaphosphoric acid in an enzymatic recycling method using glutathione reductase, as previously described.(10) For cellular GPx activity we used a modified technique of Lawrence and Burke.(11) Briefly, GSH and hydrogen peroxide were used as substrates, and oxidized glutathione (GSSG) was monitored through NADPH oxidation with glutathione reductase. The final concentrations of the reagents in the reaction mixture were 50 mm potassium phosphate, pH 7.0, 1 mm EDTA, 1 mm NaN_3, 0.2 mm NADPH, 1 unit·ml^{-1} GSSG reductase, 4 mm GSH, and 0.25 mm H_2O_2. The change in absorbance at 340 nm was recorded. GPx activity was calculated using an extinction coefficient of $6.22 \cdot 10^{-3}$ μm $^{-1} \cdot cm^{-1}$ for NADPH at 340 nm. Specific activities are expressed as nmol of NADPH·$min^{-1} \cdot mg^{-1}$ protein. Protein content was determined using the Bio-Rad protein assay kit. Bovine serum albumin was used as a protein standard.

Balloon Angioplasty and Stenting

BAS was performed in 18 to 22 week-old male mice as described previously.(12) All operative

procedures involved grafting a thoracic aortic segment from a female donor mouse to the carotid artery of a male littermate recipient. To prevent thrombosis, mice received aspirin 10 mg/kg/d in the drinking water, beginning one week prior to and continuing throughout the experimental period. All mice were anesthetized with pentobarbital sodium (50 mg/kg body weight, given intraperitoneally). The thoracic aorta of the donor female mouse, was isolated from the arch to the diaphragm. A small transverse arteriotomy was made just superior to the diaphragmatic outlet. A stainless-steel stent (Nanointerventions Ltd) 2.5 x 0.6 mm in dimension was crimped onto a 1.25 x 13 mm balloon angioplasty catheter (Invatec International) and guided retrograde to the mid portion of the descending thoracic aorta and the balloon inflated to 8 atmospheres pressure for 30 seconds, deploying the stent to a final internal diameter of 1.25 mm (balloon-to-vessel ratio of 1.5:1). When balloon angioplasty alone was performed, no stent was used. The aorta was harvested by sealing the intercostal branch vessels with electrocautery. In the recipient (male) mouse, the right common carotid artery was isolated ligated, and divided between ties at its midpoint. Polyethylene cuffs (0.65 mm diameter, Portex Ltd) were placed over the ends of the vessel and anchored by microhemostatic clamps (Aesculap). Sutures at the ends of the artery were removed, and the artery everted over the cuffs and secured with sutures. The stented aorta from the donor mouse was grafted by sleeving the ends of the aorta over the 2 ends of the carotid artery and ligating them. Vigorous pulsations within the conduit vessel confirmed a successful procedure.

Gene Transfer

Freshly harvested vessels were incubated in a total of 1×10^{11} viral particles of AdGrx1 or AdGFP in 300 μL for 30 minutes at 37°C prior to implantation. Successful gene transfer was confirmed by immunohistochemistry on aortic sections for anti-GFP.

Tissue preparation, Histology and Lesion Quantification

Mice were euthanized 28 days following the stent procedure. The thoracic cage was removed and the animal perfused with phosphate buffered saline solution (PBS) for 2 minutes. The entire aorta and stent graft were exposed and the periadventitial tissue and scar tissue dissected and removed. Subsequently tissue was removed fresh for biochemical assays or mice were perfusion fixed in situ with 4% phosphate-buffered paraformaldehyde.

Aorta and stented vessels were excised, fixed in paraformaldehyde overnight, dehydrated in graded ethanol solution, and paraffin embedded or removed fresh and snap frozen in OCT. For stent analysis vessels were excised, fixed in paraformaldehyde overnight, and subsequently embedded into glycol methacrylate resin (Technovit 8100, TAAB Laboratories) for histomorphometry, or methyl methacrylate resin (Technovit 9100, TAAB Laboratories) for immunohistochemistry, according to the manufacturer's instructions. Four transverse sections were cut through each stent using an Isomet 5000 diamond-coated rotary saw and polished (to 5-10μm) using a Metaserv 2000 polisher (Buehler, UK).

For histomorphometric analysis, sections were stained with hematoxylin and eosin or Masson trichrome. Lesions were quantified for total vessel area (area inside the external elastic lamina), neointimal area (area inside the internal elastic lamina, minus stent struts, minus lumen), lumen, and stent expansion (area inside a polygon connecting the midpoint of each stent strut). In some vessels, measurements of neointimal thickness were performed by measuring the perpendicular distance from lumen to internal elastic lamina at the mid point between stent struts on each section (4-6 measurements per section; 4 sections per vessel to generate n=1).

Aortic atherosclerosis lesion area was determined as described previously.(13) The heart and full length of the aorta-to-iliac bifurcation was exposed and dissected carefully from any surrounding tissues. Aortas were then opened along the ventral midline and dissected free of the animal and pinned out flat, intimal side up, onto black wax. Aortic images were captured with a digital camera (DMC1) mounted on a Leica MZ6 stereomicroscope and analyzed using Fovea Pro (Reindeer Graphics, Asheville, NC). Percent lesion area was calculated as total lesion area divided by total surface area.

For the quantification of atherosclerotic lesion sizes in paraffin-embedded aortic root sections, Masson–Goldner staining was performed according to the manufacturer's instructions (Merck). The mean value for atherosclerotic lesion size was calculated from three sections; starting from the first section showing all three complete aortic cusps, each of the next two sections was taken 144 µm distally to the previous one. Lesion size was quantified with ImagePro Plus software (MediaCybernetics, MD). The infiltration of macrophages/monocytes into aortic lesions was analysed as absolute positive staining area using an antibody against the Mac-3 antigen (rat anti-mouse Mac-3 antibody; BD Pharmingen). The level of fibrosis within atherosclerotic lesions was quantified by immunostaining against the extracellular matrix component collagen type IV (rabbit anti-mouse collagen type IV antibody; Chemicon International). Smooth muscle cells were visualized by staining with and Cy3 (indocarbocyanine)-conjugated mouse monoclonal anti-α smooth muscle actin antibody (Sigma; cat. no. C6198). Absolute Mac-3, collagen type IV and α smooth muscle actin were quantified using a Leica fluorescence microscope.

En Face X-Gal Staining

The procedure for en face preparation was similar to that described previously.(14) Briefly, freshly harvested vessel segments were incubated at 37°C for 3 hours in PBS containing 1mg/mL X-Gal (Sigma), 5mml/L potassium ferricyanide, 5mmol/L potassium ferrocyanide and 2 mmol/L $MgCl_2$. Vessel segments were rinsed with 3% DMSO in PBS and mounted with the endothelium up on paraffin base. Endothelial blue staining (intensity x area) was measured from high power (70x mag) images of the luminal side of the vessel using Image Pro Plus software (Media Cybernetics, Silver Springs, Maryland). Mean blue colour signal was calculated from 4 separate high power fields to produce n=1.

Oxidative fluorescent microtopography

Superoxide was detected in the layers of the vessel wall using fluorescent probe dihydroethidium as described previously. Fresh segments of upper descending thoracic aorta were frozen in OCT compound.

Cryosections (30µm) were incubated with Krebs-HEPES buffer for 30 minutes at 37°C with or without 1mmol/l L-NAME, 50µmol/l apocynin or 50U/ml superoxide dismutase (Sigma), followed by 5 minutes dark incubation with 2µmol/l dihydroethidium (DHE; Molecular Probes). Images were obtained on a confocal microscope (Bio-Rad MRC-1024 laser; filter settings: excitation filter 488 nm; emission filter 550 nm). Endothelial 2-hydroxyethidium fluorescence (intensity x area) was measured from high power (60x mag) images of the luminal side of the internal elastic lamina using Image Pro Plus software (Media Cybernetics, Silver Springs, Maryland). Analysis was performed blind to the samples identity. Mean fluorescence was calculated from 4 separate high power fields from each quadrant to produce n=1.

Lucigenin and luminol-enhanced chemiluminescence

Total aortic superoxide and hydrogen peroxide was measured by lucigenin and luminol-enhanced chemiluminescence respectively as described previously.(15) Aortas were harvested flushed with Krebs-HEPES buffer, opened longitudinally and divided into halves. Vessels were gassed with 95% oxygen/5% carbon dioxide in warmed Krebs-HEPES buffer for 30 minutes before measurements of chemiluminescence in an FB12 luminometer (Berthold Detection Systems, Germany) using using 5 µmol/L lucigenin for superoxide generation. One half of each vessel was incubated in L-NAME (1 mmol/L) (Sigma-Aldrich) to determine the contribution of eNOS and nNOS. Hydrogen peroxide generation was achieved by assessment of the uric acid (1 mmol/L) inhibitable luminol (100mmol/L) chemiluminescence. After measuring baseline readings for 4 minutes, samples were equilibrated and dark adapted for 5 mins, and chemiluminescence was recorded for 10 minutes. Recordings were performed blinded to the samples identity. Results were expressed as counts per second per milligram of tissue dry weight.

Electron paramagnetic resonance (EPR) spectroscopy

EPR spectroscopy was used to quantify vascular NO production according to previously described and validated methods.(16) In brief, freshly harvested aortas (n = 4 to 8 per group) were stimulated with

calcium ionophore (A23187; 1 μmol/L) in 250μl Krebs-HEPES buffer then incubated with colloid $Fe(DETC)_2$ (285 μM) at 37°C for 90 minutes. After incubation, aortas were snap frozen in a column of Krebs-HEPES buffer in liquid nitrogen and EPR spectra were obtained using an X-band EPR spectrometer (Miniscope MS 200, Magnettech, Germany). Signals were quantified by measuring the total amplitude, after correction of baseline, and after subtracting background signals from incubation with colloid $Fe(DETC)_2$ alone.

Cell culture

Human coronary artery SMCs (Lonza, Walkersville, MD, passage #3-6) were propagated in SmGM-2 growth media (Lonza) containing 5% FBS. To induce growth arrest and the expression of differentiation genes, SMCs were serum starved in basal media (SmBM) for 72 hours, according to conventional protocols.(17) *In vitro* ROS1 inhibition studies were completed by adding 40uM genistein or crizotinib 1uM or 10uM to the cell culture media, as previously described.(13) For knockdown experiments, VSMCs were transfected with 25 nM of anti-ROS1, anti-Grx1 or high-GC control siRNA (Ambion, Silencer Select, catalog # 4390825, 4392420 and 4390843 respectively) using the high-efficiency Amaxa Nucleofector system (Lonza, protocol U-025). For adenoviral overexpression of Grx1 we used a doxyycline-controlled Tet-On adenoviral gene expression vector carrying a loxp cassette in its multi-cloning site (a generous gift from Dr Reto Asmis, University of Texas San Antonio) as described previously.(18) Plates were harvested at 80% confluence for RNA and protein analysis or used for subsequent *in vitro* analysis.

Primary aortic SMCs from experimental animals were cultivated as described by Ross.(19) In short, following balloon angioplasty mouse thoracic aortas were removed and washed with RPMI 1640 medium. The intima and inner two thirds of the media were carefully dissected from the vessel under an anatomic microscope, cut into pieces (1x1x0.1 mm), and planted onto a gelatin-coated (0.02%) plastic bottle (Falcon). The bottle was incubated upside down at 37°C in a humidified atmosphere of 95% air/5% CO_2 for 3 hours, and then medium supplemented with 20% FCS, penicillin (100 U/mL), and streptomycin

(100 µg/mL) was slowly added. Cells were incubated at 37°C for 10 to 14 days and passaged by treatment with 0.05% trypsin/0.02% EDTA solution. Experiments were conducted on SMCs that had just achieved confluence.

Proliferation and motility assays

Cells were seeded at $25x10^3$ cells per well on 24-well plates in SMC growth medium and allowed to adhere overnight. The next day, cells were washed and incubated in SMC starvation medium for 48 hours followed by stimulation with agonists for various time intervals indicated in the Figure Legends. Cells were then trypsinized and counted in a hemocytometer.

Migration assays were performed using the modified Boyden chamber assay: SMCs (1 × 104 cells/ml, in 200 µl) were placed in the upper chamber in the absence or presence of stimulus in the lower chamber. After 6 hours of incubation, the cells were removed from the upper face of the Transwell membrane and those in the underside of the membrane were fixed and stained with 0.5% toluidine blue in 4% paraformaldehyde. Migration was quantified with an inverted phase contrast microscope (Leica) by calculating the total average number of cells in six random 200x magnification fields per well. The migration index was obtained by comparing the values in the experimental groups to the unstimulated control. All assays were done in triplicate and three separate cell harvests were assessed.

Survival assay

For Caspase 3/7 assays, cells were seeded in a 96-well plate (4 wells per condition and 5,000 cells per well) and allowed to attach overnight, then incubated for 24 h in serum free media to induce apoptosis. Then cells were incubated for 1 in 100 µl of Caspase 3/7 Luciferase Reagent Mix (Promega, Inc, Madison WI) and total luminescence measured in a Turner 20/20 luminometer (Turner Biosystems, Inc, Sunnyvale, CA).

Quantitative Real-Time PCR

Total RNA was extracted from snap frozen tissue by pulverization/homogenization in 1mL of Trizol solution (Sigma-Aldrich, St. Louis, Missouri, USA). For cell experiments, RNA was isolated from cell lysates using the miRNeasy Mini Kit (Qiagen, Valencia, CA) according to the manufacturer's protocol. For quantitation of gene transcription, cDNA was generated with M-MuLV reverse transcriptase, and then amplified on the ABI PRISM 7900HT with TaqMan primers (Applied Biosystems, Foster City, CA) normalized to 18S internal controls, as previously described.(13) Samples were processed in duplicate, negative control reaction for each sample. Mean values were calculated from duplicate samples to produce an *n* of 1. Results from at least four animals per group were pooled to produce means and SEMs.

Immunoprecipitation and immunoblotting

Immunoprecipitations were performed on cells lysed with cell lysis buffer. Lysates were precleared with protein G agarose, and immunoprecipitation was performed with the respective antibodies at a concentration of 1 µg/ml for 24 hours at 4°C. Protein G agarose was added and incubated for an additional 2 hours. Western blotting of SDS-PAGE gels was performed with standard methodology. Aortic or stented vessel lysates ($n \geq 4$ per group) were homogenized on ice for 20 seconds in lysis buffer (50 mmol/L Tris, pH 7.5, 150 mmol/L NaCl, 0.1% SDS, 0.5% deoxycholate, 1% Nonidet P-40) containing protease inhibitors (Complete; Boehringer Mannheim) and 1 mmol/L phenylmethylsulfonyl fluoride. Protein lysates (8 µg) were resolved using SDS-PAGE and transferred to polyvinylidene difluoride membranes. Membranes were incubated with a 1:2000 mouse anti-eNOS monoclonal antibody (Transduction Laboratories) which recognizes murine and bovine eNOS, 1:1000 rabbit anti-phosporylated ROS1 which recognizes activated ROS1 (Santa Cruz Biotechnology, CA) followed by a 1:2500 dilution of rabbit anti-mouse horseradish peroxidase–conjugated secondary antibody (Promega). Protein bands were analyzed by band intensity.

Biotinylated GSH Ester and Detection of S-Glutathiolated Proteins

Biotinylated GSH ester was made by mixing 25 mM sulfo-NHSbiotin with 25 mM GSH ethyl ester in 50 mM NaHCO3 at pH 8.5 for 2 h followed by the addition of 125 mM NH4HCO3 at pH 8.5 for 1 h. Biotinylated GSH ester (250μM) was preincubated with VSMCs in culture for 1 h. At each time point the cells were washed three times with cold phosphate buffer and lysed in buffer (Tris-HCl, pH 7.4, 1% Nonidet P-40, 150 mM NaCl, 50 _M diethylenetriaminepentaacetic acid,
2 mM phenylmethylsulfonyl fluoride) containing 10 mM N-ethylmaleimide to block further thiol reactions. Approximately 1 mg of protein was passed through a PD-10 Sephadex-G25 column to eliminate the excess low molecular weight biotin products. The proteins were mixed with streptavidin-Sepharose beads for 1 h. The beads were washed five times with lysis buffer with 0.1% SDS, and the final precipitate was incubated for 10 min with 40 μl of elution buffer (lysis buffer + 20 mM DTT) to release *s*-glutathiolated proteins. After adding Laemmli buffer containing 5% β-mercaptoethanol, GSS- ROS1, SHP-1 or SHP-2 was detected by immunoblotting with monoclonal anti- ROS1 antibody (Cell Signaling, SC-6348), anti-SHP-1 antibody (Cell Signaling, 3759), or anti-SHP-2 antibody (Cell Signaling, 3397). S-glutathiolated proteins were also detected directly with monoclonal anti-glutathione antibody (Virogen).

Mass Spectroscopy

c-Myc pull down fractions were precipitated with 4x's sample volume -80◦C acetone and let sit on dry ice for 1 hour, following ultracentrifugation at 10K g, 4◦C for 10 minutes. Solution phase was removed and the protein precipitate was dried in a speed vac. Each sample was reconstituted in 8M urea, 0.2% protease max (Promega), 50mM ammonium bicarbonate followed by trypsin digestion under three scenarios as to observe the cysteine state: a) no reduction, no alkylation (native) b) no reduction, alkylation using 5 mM iodoacetamide c) reduction and alkylation following standard procedure as previously reported. A Proxeon EASY-nLC and Proxeon nanospray source were interfaced to an LTQ Orbitrap Velos MS with ETD. The LC mobile phases were: A- 0.585% acetic acid 99.415% water, B- 0.585% acetic acid 99.415%

acetonitrile, where a linear gradient from 2% mobile phase B to 40% B was employed. Fragmentation was performed in a data dependent fashion on multiply charged cations (top 12 or 6 most intense) using CID alone (high/low workflow), or an alternating HCD/ETD workflow, respectively. The data was processed on a Sorcerer system using Sequest searching the human uniprot database. Strict trypsin specificity was used and data was searched with a 20ppm precursor mass tolerance later filter to less than 8ppm. The variable modifications were: K (lysine) acetylation, C (cysteine) carbamidomethyl, glutathione, cysteic acid, and M (methionine) oxidation. All spectra indicating glutathionylation were manually validated. The data was visualized using Scaffold v. 3.

Protein-Ligand Docking with Dynamics

The structure of SHP-2 protein (2SHP.pdb) was downloaded from the protein data bank (PDB) and chain A was considered for docking with glutathione (GSH). The mol file was downloaded from Drugbank and preprocessed to ensure that the input conformation does not bias the final docking results. The query ligand is first converted to a 3D structure using ChemAxon's MarvinBeans molconverter v.5.11.3. (http://www.chemaxon.com/).

SwissDock methodology[1] was used to dock glutathione to SHP-2 with side chain flexibility to get a starting point for further refinements. The active site centroid was specified to the docking program (Xcenter = 23.77, Ycenter = -21.58, Zcenter = 49.20) with the docking region of interest of 10Å around the centroid. Protein side chain flexibility was specified within 3Å of any atom of the GSH ligand in its reference binding mode.

The docked poses were further refined by energy minimization using GROMACS (version 4.5.5) software package.[2] The CHARMM force field was used and highly convergent L-BFGS minimizer with all intermolecular interactions including flexibility of both the protein and the ligand. This was done in order to relax the docked structure around its conformation which removes steric intermolecular atomic clashes and converges within the energy minimization threshold before significant torsion angle differences of the ligand take place. All the refined docking poses were scored using the r·m·r·6 criterion

with the knowledge based potential function which has been shown to discriminate native poses.[3] Selection of final poses was made based on scores and distance cutoff for glutathionation of Cys333 and Cys459 with GSH. The schematics shown in the manuscript were made for the selected poses using PyMol molecular graphics program.(20)

Lipid and Lipoprotein Analysis

Total plasma cholesterol and triglyceride concentrations were measured using enzymatic assay (Roche, Indianapolis, IN) on a Cobas Mira Plus automated analyzer (Roche, Switzerland).

SNP Information Gain Analysis

461 coronary artery disease patients who underwent bare metal stenting were recruited as previously described.(21) Genomic DNA was isolated from venous blood. One hundred and forty two polymorphisms in 121 candidate genes were assayed using the Luminex 100 flow cytometer (Luminex, Austin, TX). Primary genotyping and clinical follow up data was loaded into Weka, an open source extensible package environment for data mining and machine learning (http://www.cs.waikato.ac.nz/~ml/weka/). Attribute selection analysis was then performed in the Weka (Java) environment, using all SNPs as the attributes and using an information gain evaluator conditioned on the presence or absence of in-stent stenosis with ranker as the attribute search method.

SNP Interaction Analysis

SNP interaction analysis was performed using the Polymorphism Interaction Analysis tool to evaluate for interactions between SNP combinations in case-control genotyping association studies (PIA v2.0 available at http://www3.cancer.gov/intra/lhc/PIA2-distribution.zip).(22) PIA uses seven scoring metrics of SNP interaction and accounts for imbalance in the case and control numbers. Case based exclusion is used for missing data and n-fold cross validation can be performed. Scoring metrics for interaction comprise: % correct, sensitivity + specificity, PPV + NPV, risk ratio, odds ratio, Gini index, and absolute

probability difference. A 2-SNP interaction model was used for the analysis presented here. Monte Carlo simulation on randomly categorized data was used to estimate a q-value cutoff for significance.

Linear Regression Model

Fitting of a generalized linear regression model was done in R (http://www.r-project.org/) conditioning the presence or absence of in-stent stenosis on a score consisting of the number of at-risk alleles for both *GPX1* and *ROS1*, with a minimum of 0 and a maximum of 3 (no member of the cohort had 4 at-risk alleles).

Genome Wide Association Study Meta-Analysis

A meta-analysis was performed combining cases and controls from 4 separate cohorts comparing patients after balloon angioplasty and stenting who developed in-stent stenosis with those who did not. The methods for each individual case – control cohort are as follows:

Cardiogene: The CardioGene Study was an institutional review board (IRB) approved, prospective cohort study of 358 patients enrolled at the time of bare metal stent implantation to treat de novo, previously untreated native coronary artery lesions at William Beaumont Hospital (Royal Oak, Michigan, USA) and the Mayo Clinic (Rochester, Minnesota, USA). Methods were described previously.(23) Briefly patients were enrolled from February 2002 through September 2003 and followed for 1 year to determine in-stent stenosis outcomes. Additionally, 104 individuals were enrolled with historical in-stent stenosis in bare metal stents, with two or more episodes of restenosis in native coronary arteries. Informed consent was obtained from all patients and the protocol was approved by the NHLBI IRB as well as the IRB at each of the clinical enrollment sites. Follow-up clinical evaluation was performed via patient interview and review of all available medical records at 6 months and 12 months post-stent. In-stent stenosis was defined as clinical restenosis determined as ischemic symptoms after stent implantation and evidence of flow limitation in the treated vessel by either invasive or non-invasive testing. Follow-up angiography was not specifically performed. Genotypes were assayed using the

Affymetrix Genome-Wide Human SNP Array 6.0 platform, and genotypes were called using the Birdseed algorithm. Genotype call rates were 95% or greater for all samples. Samples with sex mismatch, first-degree relative of an included individual, and genetic outlier based upon allele sharing and principal components analysis were removed. The final sample with genotype data consisted of 407 samples, with 150 in-stent stenosis cases and 257 stented no-stenosis controls, all from European ancestry participants among which call rates and deviations from Hardy-Weinberg equilibrium for all SNPs were calculated.

GeneBank: The Cleveland Clinic GeneBank study is a single site sample repository generated from consecutive patients undergoing elective diagnostic coronary angiography or elective cardiac computed tomographic angiography with extensive clinical and laboratory characterization and longitudinal observation. Subject recruitment occurred between 2001 and 2006. Ethnicity was self-reported and information regarding demographics, medical history, and medication use was obtained by patient interviews and confirmed by chart reviews. All clinical outcome data were verified by source documentation. Coronary artery disease was defined as adjudicated diagnoses of stable or unstable angina, myocardial infarction (adjudicated definition based on defined electrocardiographic changes or elevated cardiac enzymes), angiographic evidence of 50% stenosis of one or more major epicardial vessel, and/or a history of known coronary artery disease (documented infarction, coronary disease, or history of revascularization). A subset of individuals with bare metal stents implanted prior to 2003 was analyzed in this study, numbering 348 cases of in-stent stenosis and 1,151 controls without evidence of stenosis. In-stent stenosis was defined as target vessel revascularization. Genotyping was performed using the Affymetrix Human SNP Array 6.0 platform. All patients provided written informed consent prior to being enrolled in GeneBank and the study was approved by the Institutional Review Board of the Cleveland Clinic.

DeCODE: As part of the DeCODE cohort, consecutive patients undergoing stent implantation with bare-metal stents were enrolled in Iceland at Landispitali University Hospital and University of Iceland. Patients were followed up at 1 year to confirm in-stent stenosis or stented no-stenosis status. In-stent stenosis was defined as target vessel revascularization within 1 year. All Icelandic case- and control-

samples were assayed with the Infinium HumanHap300 SNP chips from Illumina, SanDiego, CA, USA. Genotyping was carried out at deCODE genetics in Reykjavik, Iceland. SNPs assayed on the chip were excluded if they had (a) yield lower than 95% in cases or controls, (b) minor allele frequency less than 1% in the population, or (c) showed significant deviation from Hardy-Weinberg equilibrium in the controls (P-value < 0.001). Any samples with a call rate below 98% were excluded from the analysis. The final sample size consisted of 930 patients, including 240 cases of in-stent stenosis and 690 cases of stented no-restenosis. The study was approved by the National Bioethics Committee and the Data Protection Authority of Iceland, and each patient provided informed consent for participation in the study.

GENDER: The main characteristics of the GENDER population have been described previously.(24) Briefly, 3104 consecutive symptomatic patients treated successfully by balloon angioplasty and stenting for angina were included in four referral centers for interventional cardiology in the Netherlands. The follow-up protocol included a phone contact or a medical visit at the outpatient clinic at 30 days and around 9 months after stent placement. Clinical in-stent stenosis was defined as renewed symptoms requiring target vessel revascularization either by repeated angioplasty and stenting or coronary artery bypass graft surgery, by death from cardiac causes or myocardial infarction not attributable to another coronary event than the target vessel. Within the 9-month follow-up period, 346 patients developed clinical in-stent stenosis. The GWAS was performed in 325 cases of in-stent stenosis (all cases with enough quality DNA to perform the experiment) and 630 matched controls. Cases and controls were matched by gender, age and some possible confounding clinical variables for restenosis in the GENDER study, such as total occlusion, diabetes, current smoking and residual stenosis. Mean time follow-up was 9.5 years (SD 1⁄4 3 years) and 239 (28%) of patients died during the study. From the patients analyzed in the GWAS, only nine subjects (1.0%) were lost to long-term follow-up. Genotyping was conducted using the Illumina Human 610-Quad Beadchips and the Infinium II assay following manufacturer's instructions. After stringent quality control measures were applied as described previously,(24) the final data set consisted of 866 (295 cases, 571 controls) individuals and 556,099 SNPs that passed all quality-control criteria.

Statistical Analysis

Data are presented as mean ± SEM. Data were subjected to the Kolmogorov-Smirnov test to determine distribution. Groups were compared using the Mann-Whitney U test for non-parametric data or Student's t-test for normally distributed data. When comparing multiple groups data were analyzed by analysis of variance (ANOVA) with Newman-Keuls post-hoc test for parametric data or Kruskal-Wallis test with Dunns post test for non-parametric data.

Supplementary Figure Legends

Supplementary Figure 1. *GPx1* deletion in *ApoE*$^{-/-}$ mice decreases vascular GPx activity. The relative amount of GPx activity in heart, aorta and vena cava was significantly lower in *GPx1*$^{-/-}$*/ApoE*$^{-/-}$ mice compared with *GPx1*$^{+/+}$*/ApoE*$^{-/-}$. No difference was found in plasma. Intra-group comparisons. *P<0.01 vs *GPx1*$^{+/+}$*/ApoE*$^{-/-}$, n=5-8.

Supplementary Figure 2. Increased smooth muscle cell content in *GPx1*$^{-/-}$*/ApoE*$^{-/-}$ atherosclerotic lesions. Phenotypic analysis of atherosclerotic plaque in experimental animals was determined on aortic root sections. Macrophage content was measured using anti-MAC3 antibody; lipid content using Oil Red O; smooth muscle content using anti-α-actin antibody and collagen using anti-COL IV. Double white bar denotes 5μm, single white bar 50μm.

Supplementary Figure 3. Vascular Injury Response to Balloon Angioplasty and Stenting. a) The stent consists of 1 linear unit of 5 radial cells. The stent pattern is cut by YAG laser from 0.635 mm diameter 316 stainless steel hypotube. The overall length is 2.5 mm, and the strut dimensions are 70 µm wide after polishing. **b**) (i) In the donor mouse the stent is crimped onto a 1.25 mm balloon angioplasty catheter and the catheter advanced retrograde up the thoracic aorta. (ii) The balloon is inflated to 8 atmospheres pressure for 30 seconds and the balloon catheter is retracted. In the recipient mouse the carotid artery is ligated at its midpoint, divided between ties, and cuffs placed over the ends. The vessel and cuff handle are fixed using microhemostatic clamps, the free ends of the artery everted over the cuffs and secured onto the cuff using 8-0 silk sutures. (iii) The harvested stented vessel is grafted by sleeving the ends over the artery cuffs and securing them with 8-0 silk sutures. (iv) The hemostatic clamps are removed and vigorous pulsations are seen within the stent graft. **c**) Quantitative histomorphometry of vessel sections showed that total vessel wall area and lumen area were not significantly different between groups. The extent of vascular injury caused by stent deployment is an important determinant of neointima formation. There were no differences between groups in either stent expansion or mean Schwartz vessel injury score between groups. **d)** X-gal staining for β-Gal positive cells identifies uniform

circumferential staining for endothelial cells in both *GPx1*$^{-/-}$*/ApoE*$^{-/-}$*/LacZ*$^{+}$ and *GPx1*$^{+/+}$*/ApoE*$^{-/-}$*/LacZ*$^{+}$ mice aorta. Black bar represents 100μm. Blue color indicates β-Gal positive cells

Supplementary Figure 4 *GPX1* and *ROS1* single gene variants independently and additively predict in-stent stenosis in humans. Evidence of an additive allele dose effect using a linear regression model based on the number of at-risk alleles of *GPX1* and *ROS1.*

Supplementary Figure 5. Basal levels of ROS1 Expression in Tissues and Cells. a) Caput Epididymis was used as the tissue positive control. ROS1 was detected in visceral fat, heart, kidney, large intestine (L.I., *GPx1*$^{-/-}$*/ApoE*$^{-/-}$ only), lung, small intestine (S.I.) and skeletal muscle (S.M.) at low levels. Notably ROS1 was not expressed in vascular tissues aorta, carotid or vena cava. ROS1 was not detectable in liver or spleen. **b)** Cells from experimental cell lines were cultured for qRT-PCR measurement of ROS1. HCC78 cancer cell line known to overexpress ROS1 was used as a positive control. ROS1 was detectable in fibroblasts and vascular smooth muscle cells but not endothelial cells (serum-fed or serum-starved), neutrophils or myocytes. **ROS1 regulates basic VSMC fates. c)** In primary aortic VSMCs from experimental animals we found that migration was significantly higher in *GPx1*$^{-/-}$*/ApoE*$^{-/-}$ VSMCs compared to control *GPx1*$^{+/+}$*/ApoE*$^{-/-}$. siROS1, genistein and crizotinib significantly decreased migration in *GPx1*$^{-/-}$*/ApoE*$^{-/-}$ mice but not in *GPx1*$^{+/+}$*/ApoE*$^{-/-}$ controls indicating that the phenotype was dependent on GPX1 deficiency. When siROS1 and genistein or crizotinib were used in combination there was no further benefit in reduction in migration, suggesting that these two agents share a common pathway. Daidzein, the structural analogue of genistein with similar antioxidant effects but no effect on tyrosine kinase inhibition, did not inhibit proliferation in *GPx1*$^{-/-}$*/ApoE*$^{-/-}$ cells. Addition of siROS1 to daidzein showed a similar reduction in proliferation to siROS1 alone. **d)** *GPx1*$^{-/-}$*/ApoE*$^{-/-}$ cells had decreased ability to survive compared to *GPx1*$^{+/+}$*/ApoE*$^{-/-}$ primary aortic SMCs. siROS1, genistein or crizotinib with or without siROS1 in *GPx1*$^{+/+}$*/ApoE*$^{-/-}$ cells decreased survival to similar levels to *GPx1*$^{-/-}$*/ApoE*$^{-/-}$. *P<0.05 vs *GPx1*$^{+/+}$*/ApoE*$^{-/-}$. ł P<0.05 vs controlled scrambled.

Supplementary Figure 6. *GPx1* deletion dependent intracellular accumulation of GSH regulates migration and apoptosis. a) In primary aortic VSMCs from *GPx1*$^{+/+}$*/ApoE*$^{-/-}$ animals migration was inhibited by siROS1 when cells were treated with high concentrations of GSH, while *GPx1*$^{-/-}$*/ApoE*$^{-/-}$ cells were not affected. Adenoviral overexpression of glutaredoxin 1 inhibited migration in both groups suggesting migration was mediated by protein *s*-glutathiolation. (*P <0.05 vs control; †P <0.05 vs AdGFP). **b)** Addition of GSH to *GPx1*$^{+/+}$*/ApoE*$^{-/-}$ VSMCs decreased apoptosis that could be partially reversed by the addition of siROS1 or AdGrx1. (*P <0.05 vs control; †P <0.05 vs +GSH).

Supplementary Table 1. **Lipid Profiles and Weights of Experimental Mice**

	***GPx1*$^{+/+}$*/ApoE*$^{-/-}$**	***GPx1*$^{-/-}$*/ApoE*$^{-/-}$**	***GPx1*$^{+/+}$*/ApoE*$^{-/-}$ + Crizotinib**	***GPx1*$^{-/-}$*/ApoE*$^{-/-}$ + Crizotinib**
Total Cholesterol	1312±211	1235±113	1333±139	1292±211
HDL-Cholesterol	95±13	106±11	101±13	99±16
Triglycerides	213±121	222±103	200±100	221±113
Body Weights	29±3.4	28±6.1	28±8.2	27±4.9

Serum lipid values are expressed in mg/dl, and body weights in grams.

Supplementary Table 2. **Increased smooth muscle cell content in *GPx1$^{-/-}$/ApoE$^{-/-}$* atherosclerotic lesions.**

	GPx1$^{+/+}$/ApoE$^{-/-}$	***GPx1$^{-/-}$/ApoE$^{-/-}$***	***GPx1$^{+/+}$/ApoE$^{-/-}$*** **+ Crizotinib**	***GPx1$^{-/-}$/ApoE$^{-/-}$*** **+ Crizotinib**
Number of mice per group	6	6	7	8
Macrophage, (μm^2)	15±6	16±6	16±9	17±10
Lipid, (mm^2)	0.15±0.05	0.19±0.05	0.16±0.03	0.15±0.04
SMC, (% plaque)	22±6.3	38±12*	23±9	24±13
Collagen, (% plaque)	33±13	35±16	29±12	31±14

Phenotypic analysis of atherosclerotic plaque in experimental animals was determined on aortic root sections. Macrophage content was measured using anti-MAC3 antibody; lipid content using Oil Red O; smooth muscle content using anti-α-actin antibody and collagen using anti-COL IV. *denotes $P<0.05$ compared with other groups

Supplementary Table 3. **Information Gain Analysis**

Rank	Symbol	Name	Nucleotide Change	Peptide Change	Rs ID	Information Gain
1	F3	Coagulation Factor III	1-505A>G	n/a	rs1361600	0.0148
2	BCHE	Butyrylcholinesterase	1699G>A	Ala567THr	rs1803274	0.0132
3	INSR	Insulin receptor	2946-713C>A	n/a	rs2860172	0.0121
4	TNFSF4	Tumor necrosis factor ligand superfamily, member 4	153+331T>C	n/a	rs3850641	0.0118
5	GPX1	Glutathione peroxidase	559C>T	Pro200Leu	rs1050450	0.0115
6	ROS1	v-Ros avian UR2 sarcoma virus oncogene homolog 1	6637G>C	Asp2213Asn	rs529038	0.0109
7	THBD	Thrombomodulin	1418C>T	Ala473Val	rs1042579	0.0103
8	CCL11	Chemokine, CC motif, ligand 11	67G>A	Ala23Thr	rs3744508	0.0098
9	OLR1	Low density lipoprotein, oxidized, receptor 1	501G>C	Lys167Asn	rs11053646	0.0091
10	HMOX1	Heme oxygenase 1	0.4094613A>T	n/a	rs2071746	0.0090

Information gain analysis from a candidate gene study in ISR confirms SNVs in *GPX1* and *ROS1* as informative attributes for the prediction of ISR.

Supplementary Table 4. **Peptide Mass Fingerprinting of ROS1 Immunoprecipitate**

Identified Proteins	MW
Proto-oncogene tyrosine-protein kinase ROS	264 kDa
Polyadenylate-binding protein 1	**71 kDa**
Heterogeneous nuclear ribonucleoproteins A2/B1	37 kDa
Protein TFG	43 kDa
Nucleolin	**77 kDa**
RNA-binding motif protein, X chromosome	42 kDa
60S ribosomal protein L13	24 kDa
40S ribosomal protein S18	18 kDa
THO complex subunit 4	27 kDa
Surfeit locus protein 6	41 kDa
40S ribosomal protein S8	24 kDa
40S ribosomal protein S19	16 kDa
60S ribosomal protein L8	28 kDa
Cleavage and polyadenylation specificity factor subunit 5	26 kDa
60S ribosomal protein L19	23 kDa
60S ribosomal protein L23a	18 kDa
40S ribosomal protein S25	14 kDa
U1 small nuclear ribonucleoprotein A	31 kDa
60S ribosomal protein L36	12 kDa
60S ribosomal protein L6	33 kDa
60S ribosomal protein L18	22 kDa
Tubulin alpha-1A chain	50 kDa
DNA-binding protein A	40 kDa
RNA-binding protein FUS	53 kDa
40S ribosomal protein S6	29 kDa
60S ribosomal protein L35	15 kDa
40S ribosomal protein S23	16 kDa
60S ribosomal protein L27a	17 kDa
Small nuclear ribonucleoprotein-associated proteins B and B'	25 kDa
Heterogeneous nuclear ribonucleoprotein A3	40 kDa
60S ribosomal protein L26-like 1	17 kDa
60S ribosomal protein L36a	12 kDa
Histone H1.2	21 kDa
Heterogeneous nuclear ribonucleoprotein D-like	46 kDa
60S ribosomal protein L27	16 kDa

60S ribosomal protein L3	46 kDa
Histone H2A type 1-A	14 kDa
Nucleophosmin	33 kDa
78 kDa glucose-regulated protein	72 kDa
UPF0568 protein C14orf166	28 kDa
40S ribosomal protein S4, X isoform	30 kDa
Small nuclear ribonucleoprotein Sm D2	14 kDa
Histone H1.1	22 kDa
Elongation factor 1-alpha 1	50 kDa
60S ribosomal protein L29	18 kDa
Glyceraldehyde-3-phosphate dehydrogenase	36 kDa
60S ribosomal protein L32	16 kDa
40S ribosomal protein S30	7 kDa
Small nuclear ribonucleoprotein Sm D3	14 kDa
Src homology region 2 domain-containing phosphatase-1	**68 kDa**
Src homology region 2 domain-containing phosphatase-2	**68 kDa**
60S ribosomal protein L24	18 kDa
Titin	3816 kDa
Actin, aortic smooth muscle	42 kDa

HEK 293T cells transfected with myc-ROS1 were treated with diamide to induce Cys activation and then GSH to induce and DTT to reduce *s*-glutathiolation. ROS1 was immunoprecipitated and the precipitate subjected to peptide mass fingerprinting to identify proteins physically interacting with ROS1 protein that may have been glutathiolated. Highlighted in bold are those proteins between 55-90kDa, the molecular weights between which we identified *s*-glutathiolation in ROS1 IP on immunoblot.

References

1. Hu YJ, and Diamond AM. Role of glutathione peroxidase 1 in breast cancer: loss of heterozygosity and allelic differences in the response to selenium. *Cancer research.* 2003;63(12):3347-51.
2. Schlaeger TM, Bartunkova S, Lawitts JA, Teichmann G, Risau W, Deutsch U, and Sato TN. Uniform vascular-endothelial-cell-specific gene expression in both embryonic and adult transgenic mice. *Proc Natl Acad Sci U S A.* 1997;94(7):3058-63.
3. Ai D, Chen C, Han S, Ganda A, Murphy AJ, Haeusler R, Thorp E, Accili D, Horton JD, and Tall AR. Regulation of hepatic LDL receptors by mTORC1 and PCSK9 in mice. *The Journal of clinical investigation.* 2012;122(4):1262-70.
4. King JY, Ferrara R, Tabibiazar R, Spin JM, Chen MM, Kuchinsky A, Vailaya A, Kincaid R, Tsalenko A, Deng DX, et al. Pathway analysis of coronary atherosclerosis. *Physiol Genomics.* 2005;23(1):103-18.
5. Shannon P, Markiel A, Ozier O, Baliga NS, Wang JT, Ramage D, Amin N, Schwikowski B, and Ideker T. Cytoscape: A Software Environment for Integrated Models of Biomolecular Interaction Networks. *Genome Research.* 2003;13(11):2498-504.
6. Cline MS, Smoot M, Cerami E, Kuchinsky A, Landys N, Workman C, Christmas R, Avila-Campilo I, Creech M, Gross B, et al. Integration of biological networks and gene expression data using Cytoscape. *Nat Protocols.* 2007;2(10):2366-82.
7. Smoot ME, Ono K, Ruscheinski J, Wang P-L, and Ideker T. Cytoscape 2.8: new features for data integration and network visualization. *Bioinformatics.* 2011;27(3):431-2.
8. Saito R, Smoot ME, Ono K, Ruscheinski J, Wang P-L, Lotia S, Pico AR, Bader GD, and Ideker T. A travel guide to Cytoscape plugins. *Nat Meth.* 2012;9(11):1069-76.
9. Vailaya A, Bluvas P, Kincaid R, Kuchinsky A, Creech M, and Adler A. An architecture for biological information extraction and representation. *Bioinformatics.* 2005;21(4):430-8.
10. Baker MA, Cerniglia GJ, and Zaman A. Microtiter plate assay for the measurement of glutathione and glutathione disulfide in large numbers of biological samples. *Anal Biochem.* 1990;190(2):360-5.
11. Lawrence RA, and Burk RF. Glutathione peroxidase activity in selenium-deficient rat liver. *Biochem Biophys Res Commun.* 1976;71(4):952-8.
12. Ali ZA, Alp NJ, Lupton H, Arnold N, Bannister T, Hu Y, Mussa S, Wheatcroft M, Greaves DR, Gunn J, et al. Increased in-stent stenosis in ApoE knockout mice: insights from a novel mouse model of balloon angioplasty and stenting. *Arterioscler Thromb Vasc Biol.* 2007;27(4):833-40.
13. Chun HJ, Ali ZA, Kojima Y, Kundu RK, Sheikh AY, Agrawal R, Zheng L, Leeper NJ, Pearl NE, Patterson AJ, et al. Apelin signaling antagonizes Ang II effects in mouse models of atherosclerosis. *J Clin Invest.* 2008;118(10):3343-54.
14. Xu Q, Zhang Z, Davison F, and Hu Y. Circulating progenitor cells regenerate endothelium of vein graft atherosclerosis, which Is diminished in ApoE-deficient mice. *Circ Res.* 2003.
15. Alp NJ, Mussa S, Khoo J, Guzik TJ, Cai S, Jefferson A, Rockett KA, and Channon KM. Tetrahydrobiopterin-dependent preservation of nitric oxide-mediated endothelial function in diabetes by targeted transgenic GTP-cyclohydrolase I overexpression. *J Clin Invest.* 2003;112(5):725-35.
16. Kleschyov AL, and Munzel T. Advanced spin trapping of vascular nitric oxide using colloid iron diethyldithiocarbamate. *Methods Enzymol.* 2002;359(42-51.
17. Owens GK. Regulation of differentiation of vascular smooth muscle cells. *Physiological Reviews.* 1995;75(487-517.
18. Qiao M, Kisgati M, Cholewa JM, Zhu W, Smart EJ, Sulistio MS, and Asmis R. Increased Expression of Glutathione Reductase in Macrophages Decreases Atherosclerotic Lesion Formation in Low-Density Lipoprotein Receptor–Deficient Mice. *Arteriosclerosis, Thrombosis, and Vascular Biology.* 2007;27(6):1375-82.

19. Ross R, and Kariya B. Smooth Muscle Cells in Culture. *Handbook of Physiology: Circulation, Vascular Smooth Muscle.* 1980:69-91.
20. Schrödinger L.
21. Oguri M, Kato K, Hibino T, Yokoi K, Segawa T, Matsuo H, Watanabe S, Nozawa Y, Murohara T, and Yamada Y. Genetic risk for restenosis after coronary stenting. *Atherosclerosis.* 2007;194(2):e172-8.
22. Mechanic LE, Luke BT, Goodman JE, Chanock SJ, and Harris CC. Polymorphism Interaction Analysis (PIA): a method for investigating complex gene-gene interactions. *BMC bioinformatics.* 2008;9(146.
23. Ganesh SK, Skelding KA, Mehta L, O'Neill K, Joo J, Zheng G, Goldstein J, Simari R, Billings E, Geller NL, et al. Rationale and study design of the CardioGene Study: genomics of in-stent restenosis. *Pharmacogenomics.* 2004;5(7):952-1004.
24. Sampietro ML, Trompet S, Verschuren JJW, Talens RP, Deelen J, Heijmans BT, de Winter RJ, Tio RA, Doevendans PAFM, Ganesh SK, et al. A genome-wide association study identifies a region at chromosome 12 as a potential susceptibility locus for restenosis after percutaneous coronary intervention. *Human molecular genetics.* 2011;20(23):4748-57.

Supplementary Figure 1

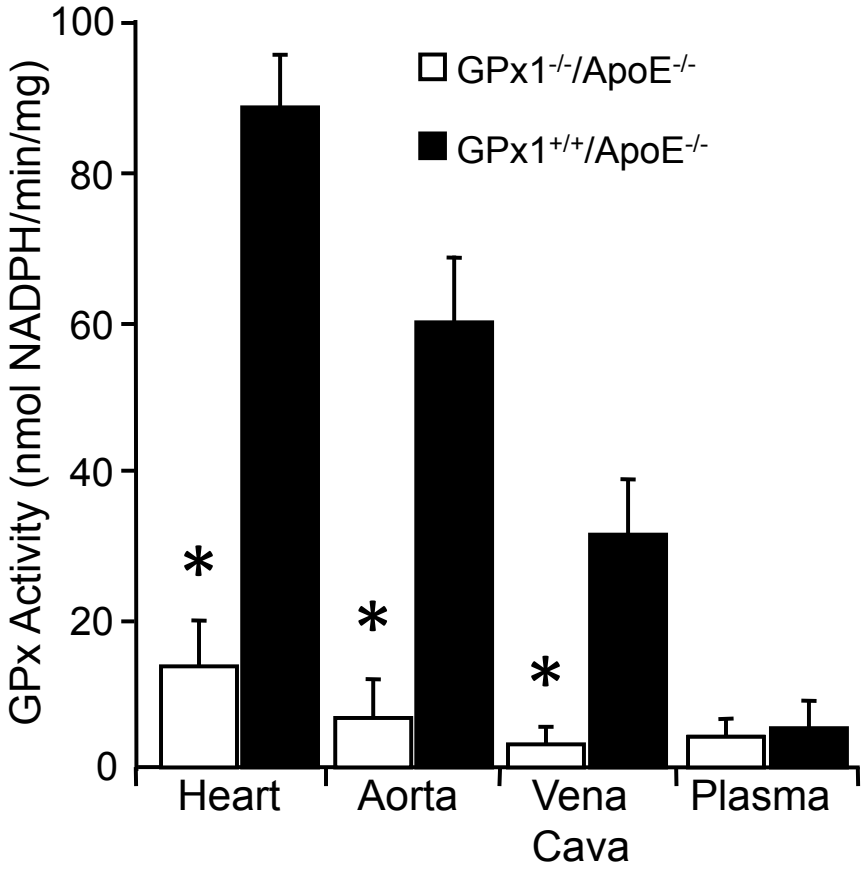

Supplementary Figure 2

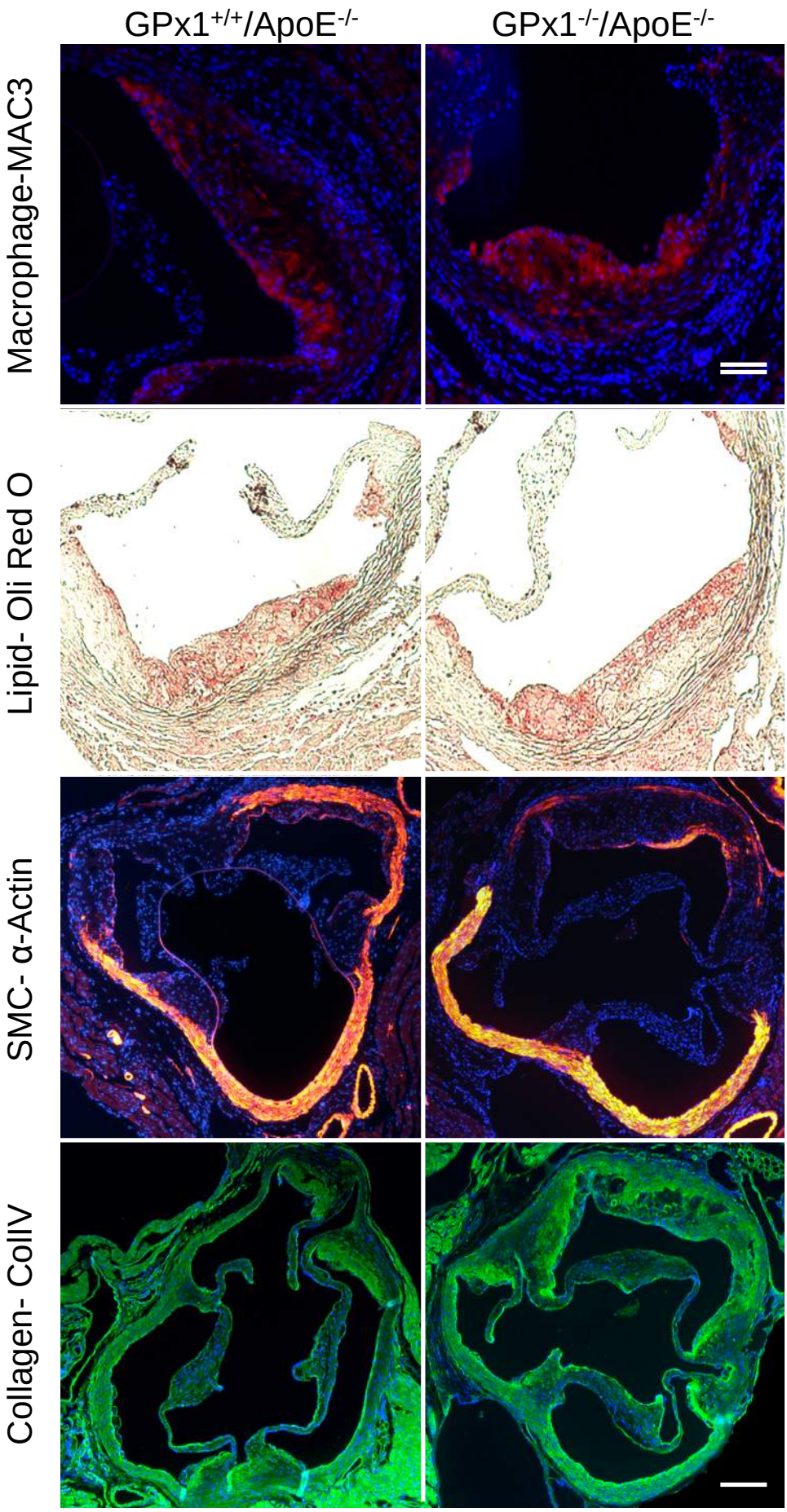

Supplementary Figure 3

A

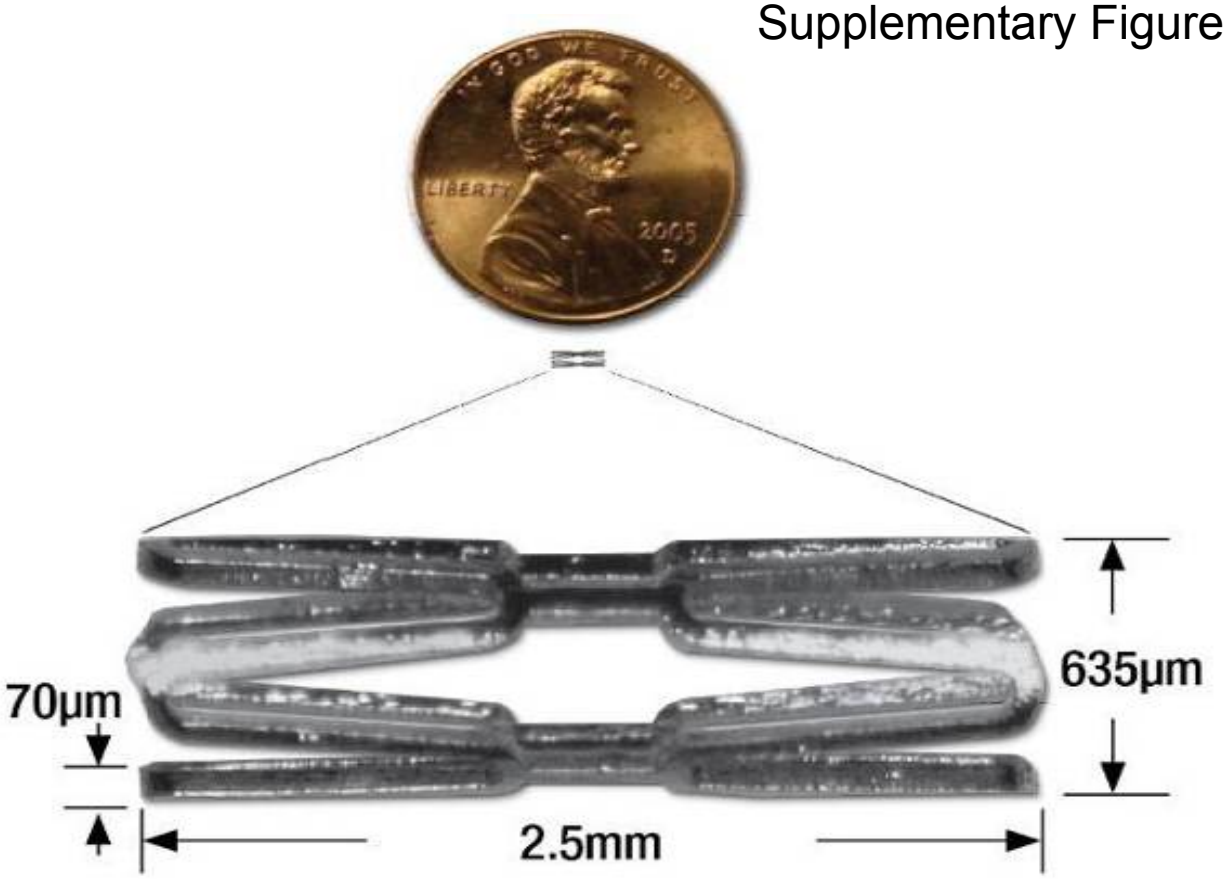

B

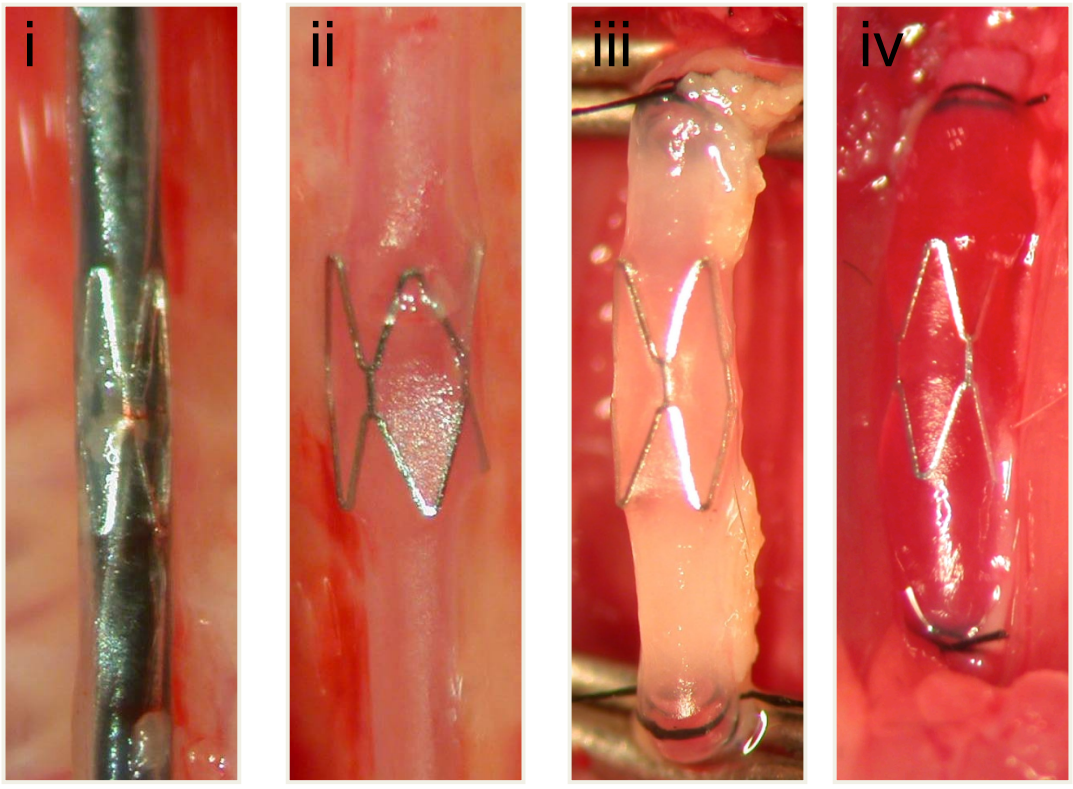

Supplementary Figure 3

C

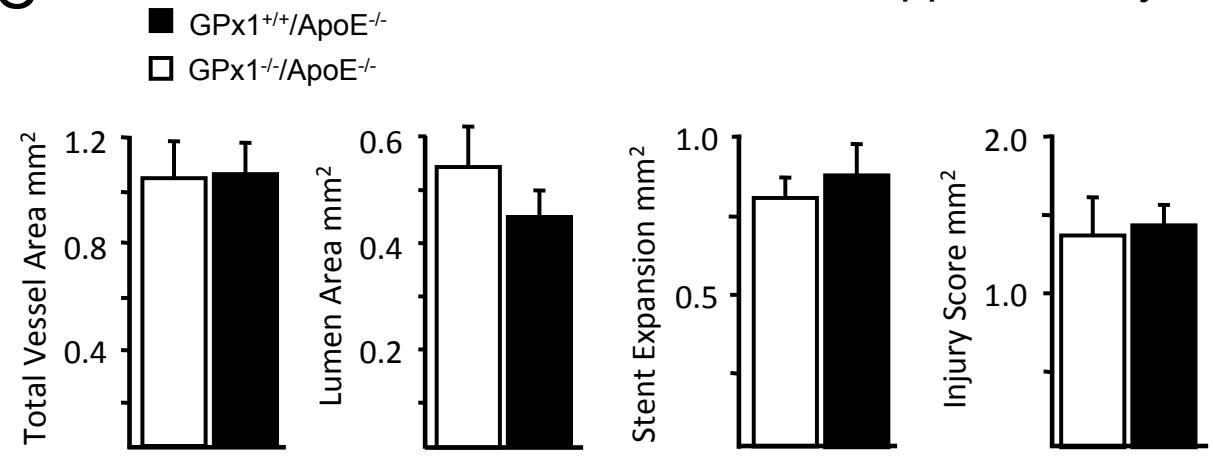

D

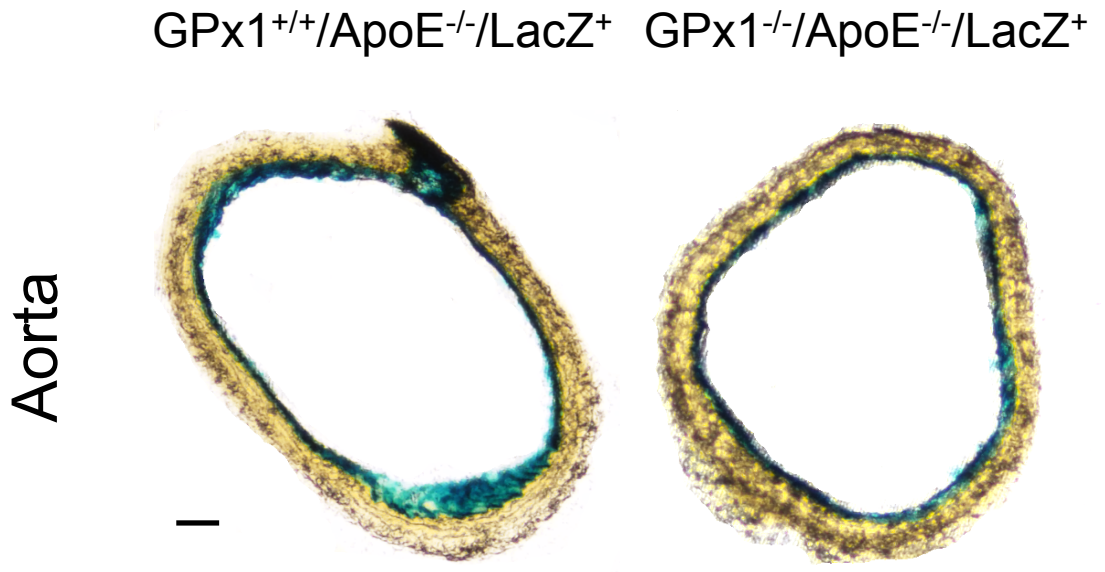

Supplementary Figure 4

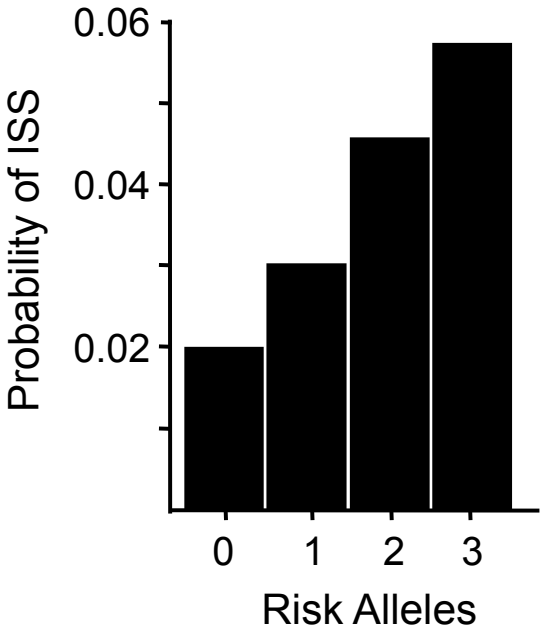

Supplementary Figure 5

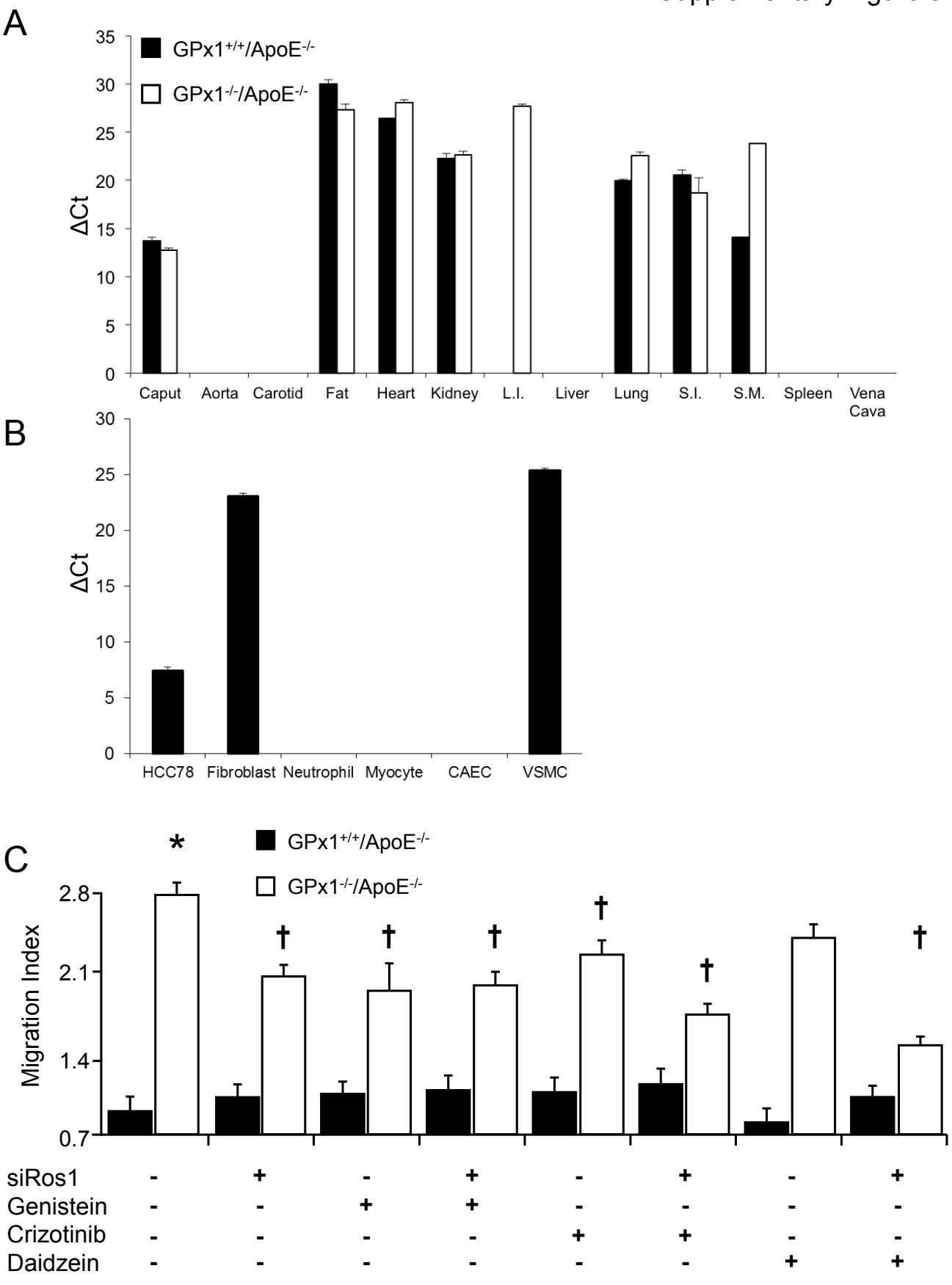

Supplementary Figure 5

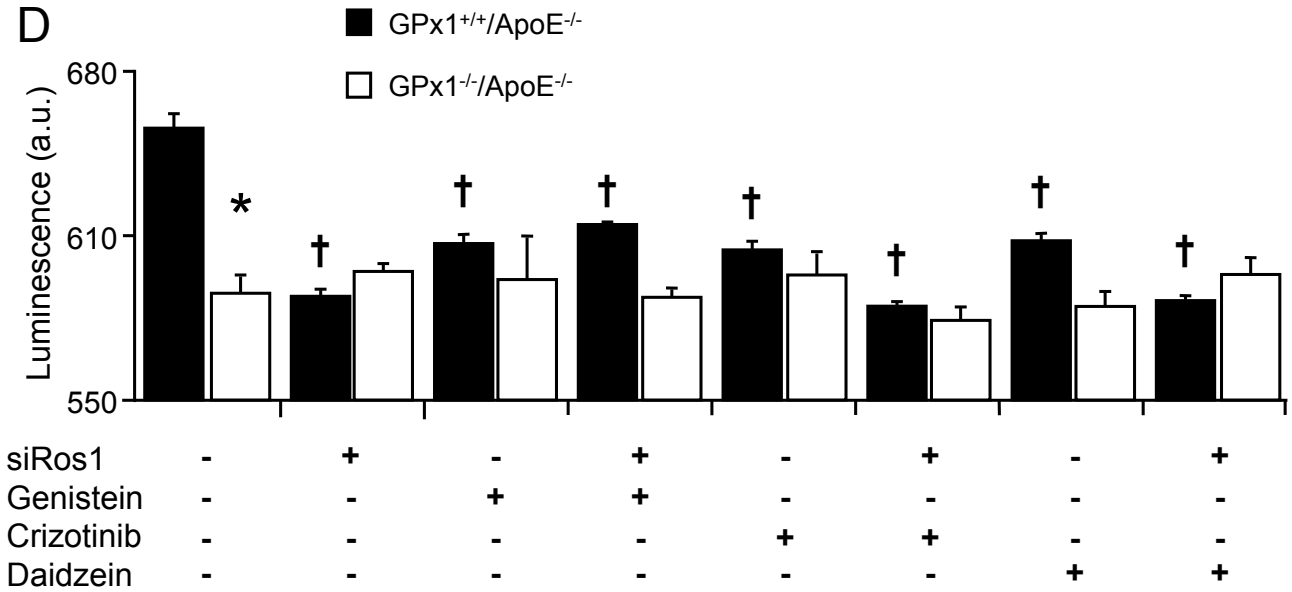

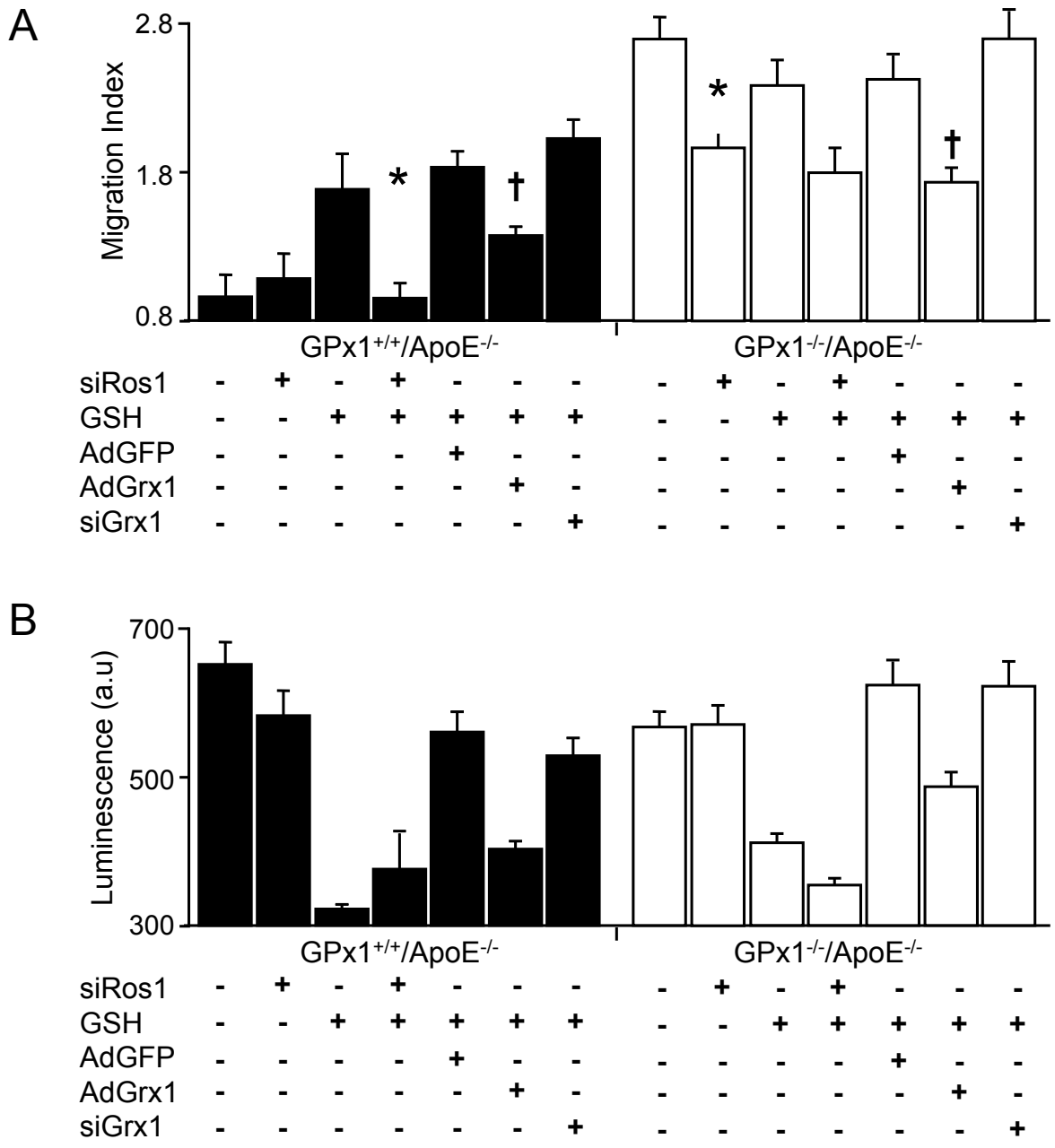
A
Migration Index
2.8
1.8
0.8
*
†
*
†
GPx1+/+/ApoE-/-
GPx1-/-/ApoE-/-
siRos1 - + - + - - - - + - + - - -
GSH - - + + + + + - - + + + + +
AdGFP - - - - + - - - - - - + - -
AdGrx1 - - - - - + - - - - - - + -
siGrx1 - - - - - - + - - - - - - +
B
Luminescence (a.u)
700
500
300
GPx1+/+/ApoE-/-
GPx1-/-/ApoE-/-
siRos1 - + - + - - - - + - + - - -
GSH - - + + + + + - - + + + + +
AdGFP - - - - + - - - - - - + - -
AdGrx1 - - - - - + - - - - - - + -
siGrx1 - - - - - - + - - - - - - +